Rare Met. (2022) 41(10):3530–3538
https://doi.org/10.1007/s12598-016-0737-0

RARE METALS
www.editorialmanager.com/rmet

Microstructure and mechanical properties of WC–(Ti, M)(C, N)–Co cemented carbides with different nitrogen contents

Han-Jie Fan, Ying Liu*, Jin-Wen Ye, Wei-Bin Qiu, Yu-Chong Qiu

Received: 12 March 2015 / Revised: 25 May 2015 / Accepted: 1 April 2016 / Published online: 7 May 2016

Abstract Three kinds of (Ti, M)(C_{1-x}, N_x) (M = Ta, Nb, W) quaternary solid-solution powders with various nitrogen contents were synthesized by carbothermal reduction–nitridation (CRN) process. Effect of nitrogen content on the microstructure and mechanical properties of WC–(Ti, M)(C_{1-x}, N_x)–Co cemented carbides fabricated by sinter-hot isostatic pressing (HIP) were systematically investigated in this paper. The results show that the nitrogen content in the carbonitride raw powders strongly influences the morphology, the grain size and the compositions of the cemented carbides. All the cemented carbides with different nitrogen contents have a similar microstructural appearance: weak core–rim structure consisting of solid-solution phase embedded in WC–Co system. It is also observed that the carbonitride solid solution could somewhat reduce the WC grain growth, and the effectiveness of refining and the rim thickness are sensitively related to the nitrogen content of (Ti, M)(C_{1-x}, N_x) solid solutions. In addition, with an increase in the nitrogen content, mechanical properties of these hard metals are enhanced, which were discussed in terms of the constituent, the microstructure and the solution behavior of the carbonitride solid solutions.

Keywords Cemented carbides; Solid-solution powders; Nitrogen content; Mechanical properties

H.-J. Fan, Y. Liu*, J.-W. Ye, W.-B. Qiu, Y.-C. Qiu
School of Materials Science and Engineering, Sichuan University, Chengdu 610065, China
e-mail: liuying5536@scu.edu.cn; liuying5536@163.com

1 Introduction

Cemented carbides consist of hard carbide grains embedded in a tough metallic matrix. Generally, conventional cemented carbides are composed of tungsten carbide particles, and these particles provide hard and brittle Co binder phase which contributes to soft and ductile properties [1, 2]. They represent a group of hard and refractory materials typically used for metal cutting, milling, turning and rock drilling, due to their unique combination of high hardness, wear resistance and moderate modulus of elasticity [3–5]. However, the performances of WC–Co cemented carbides are rapidly deteriorated when high cutting speed and elevated temperature are involved, owing to their poor oxidation resistance at elevated temperature [6]. Therefore, different cubic carbides such as TiC, TaC and NbC are commonly added in order to enhance the hardness and wear resistance of WC–Co-based cemented carbides [7]. While these different refractory metals have inconsistent physical properties, which results in the development of interfacial strain at the interface among the hard phase and the metal binder, and this strain is likely to facilitate crack initiation at the interface during cutting operations, resulting in a material with poor properties [8, 9].

In recent few decades, bunches of researchers have reported that the addition of cubic carbides in the form of pre-alloyed solid-solution materials instead of binary powders results in a material with improved properties [10]. Reference [11] showed that (Ti, W)(CN)-based solid-solution carbides in particular exhibit improved hardness and indentation toughness over conventional TiC-based cermets and other structural ceramics. Furthermore, it is known that N plays a major role in both ambient-temperature and high-temperature mechanical properties of

cermets [12]. Rafiaei et al. [4] researched that the nitrogen had a remarkable influence on the microstructure of $(Ti_{0.93}W_{0.07})C$–Ni cermets, which was believed to originate from the large affinity between carbon and nitrogen in the system. Considerable amounts of researches were done on cermets with pre-alloyed solid-solution materials. However, few literatures reported the effect of solid-solution materials on cemented carbides, and the influence of nitrogen content of carbonitride solid solution on the microstructure and mechanical properties of WC–Co cemented carbides has not been systematically researched yet.

Based on the above considerations, an innovative idea was put forward for the development of a set of WC–Co–(Ti, M)(C, N) cemented carbides with varied nitrogen contents. In this work, the microstructural characteristics of the sintered material were investigated and it focused on the changes in the composition of WC–Co–(Ti, M)(C, N) cemented carbides. It was also attempted to relate the variation of nitrogen content to the resulting microstructures and the mechanical behavior of these samples.

2 Experimental

Anatase TiO_2 (>99 wt%, <0.1 μm), Ta_2O_5 (>99 wt%, ~5.0 μm), Nb_2O_5 (>99 wt%, ~5.0 μm), WO_3 (>99 wt%, <1.0 μm) and carbon black (>99 wt%, <0.1 μm) powders were used as starting materials for synthesizing (Ti, 35Ta, 25Nb, 5W)(C_{1-x}, N_x) (denoted as (Ti, M)(C_{1-x}, N_x)) solid-solution powders by carbothermal reduction–nitridation (CRN) technique. For C and N contents in (Ti, M)(C_{1-x}, N_x) solid solutions, x was selected as 0.15, 0.20 and 0.26. Other raw materials are WC (>99.5 wt%, ~1.0 μm) and Co (>99.5 wt%, ~1.3 μm). The nominal compositions of four samples with different (Ti, M)(C_{1-x}, N_x) are listed in Table 1.

All samples were fabricated by the conventional powder metallurgy technique. Raw powders were weighted and dispersed in an ultrasonic cleaner for 10 min, and then they were wet milled with WC–8Co cemented carbides balls with diameter of 10 mm (ball-to-powder weight ratio of 10:1) in ethanol bath by a tumbling ball for 72 h. After ball milling, the slurry mixture was dried for 10 h at the temperature of 60 °C and sieved through 300 mesh. 1 wt% polyethylene glycol (PEG) was added to the mixture, and the powders were granulated before pressing into rectangular plugs. The green compacts were prepared by pressing at the uniaxial pressure of 200 MPa and dewaxed under vacuum at 350–600 °C for 8 h. Finally, vacuum sintering was carried out at 1420 °C for 1 h, with a vacuum degree of 0.1 Pa and the pressure in the dwell time was 2 MPa in argon gas.

Table 1 Nominal composition of experimental materials with different (Ti, M)(C_{1-x}, N_x)

Samples	w(WC)/wt%	w(Co)/wt%	(Ti, M)(C_{1-x}, N_x)
1	90	10	–
2	89	10	$x = 0.15$
3	89	10	$x = 0.20$
4	89	10	$x = 0.26$

The sintered specimens were grinded and polished using fine diamond polishing compounds. The phase identification was performed by X-ray diffractometer (XRD, DX-2000, China) using Cu Kα radiation with a scanning rate of 0.06 (°)·s^{-1}. The microstructure and fracture surfaces of sintered specimens were observed and analyzed by scanning electron microscopy (SEM, JSM-6490LV, Japan) in backscattered electron (BSE) mode, and the distribution of the elements was determined by X-ray energy-dispersive spectrometer (EDS) equipped to SEM. The grain sizes of WC were measured by line intercept method, while the measurement of content of core–rim structure was done using image analysis software (Image-Pro Plus 6.0).

The density of the sintered alloys was determined by the Archimedes method with an analytical balance. Three-point-bending transverse rupture strength (TRS) was conducted on a Shimadzu electron testing machine at room temperature (span of 20 mm, crosshead speed of 0.5 mm·min^{-1}). Hardness was measured by Vickers hardness tester under a constant load of 294 N. The fracture toughness was calculated by the expression derived by Shetty et al. [13].

3 Results and discussion

3.1 Powder characterization

Figure 1 shows XRD patterns and EDS spectrum of (Ti, M)(C_{1-x}, N_x) solid-solution powders with varied nitrogen contents. It can be observed that diffraction patterns consist of peaks corresponding to a single phase. Based on the experimental XRD data, it is identified as Ti(C, N) (JCPDS 42-1489). It has long been known that the (200) peak of Ti(C, N) phase is the strongest in all of its diffraction peaks, yet the peak of (111) is shown as the strongest peak in Fig. 1a. Hence, it may be deduced that the phase is not really Ti(C, N) but the (Ti, M)(C, N) solid solution. The reason for this is that the (111) plane of Ti(C, N) unit cells is composed of Ti atoms and the

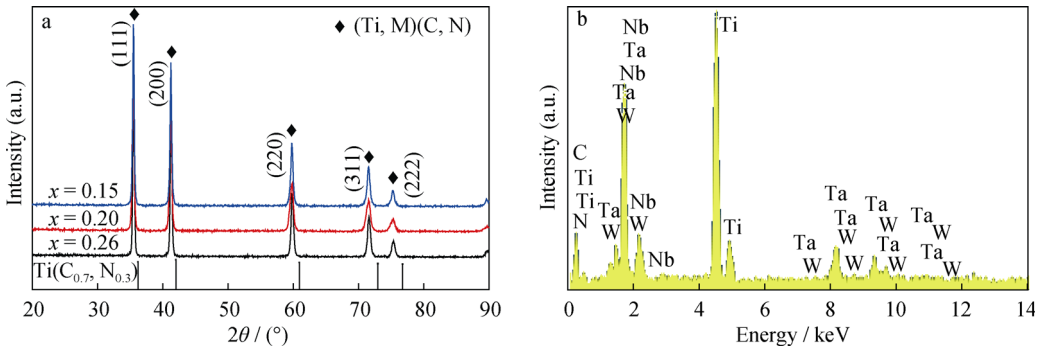

Fig. 1 XRD patterns **a** and EDS spectrum **b** of (Ti, M)(C_{1-x}, N_x) solid-solution powders with different nitrogen contents

(200) plane is occupied corporately by Ti, C and N atoms. Therefore, high probability of Ta, Nb and W atoms replacing Ti may take place on the (111) plane, rather than on the (200), which makes the $I_{(111)}/I_{(200)}$ value (the ratios between the intensities of (111) and (200) diffraction peaks) of Ti(C, N) phase increase [14]. In addition, it is found obviously that all the peaks of (Ti, M)(C_{1-x}, N_x) shift toward the lower angle compared with that of pure Ti(C, N). This result indicates that the relatively large amount of alloying elements of Ta, W, Nb, which brings severe lattice distortion, does exist in solid-solution (Ti, M)(C_{1-x}, N_x) powders and this is confirmed by the EDS result shown in Fig. 1b. All the results above indicate that a complete solid solution, (Ti, M)(C, N), is formed without any other phase and without impurities [3]. Besides, from the shift of the (111) diffraction peak of (Ti, M)(C_{1-x}, N_x) toward higher angle from 35.480° to 35.531° in the order of $x = 0.15$ to $x = 0.26$, it may be concluded that this phenomenon is directly related to the nitrogen content in (Ti, M)(C, N). As the content of nitrogen in (Ti, M)(C, N) increases, the lattice parameter decreases, which can be attributed to the smaller atomic radius of N [15].

Figure 2 shows the morphologies of (Ti, M)(C_{1-x}, N_x) solid-solution powders after CRN techniques. It can be seen that the powders, in the form of globular-like with the average grain size of about 0.5–1.0 μm, are distributed homogeneously and agglomerated partly.

3.2 Microstructure and phase composition of WC–Co–(Ti, M)(C_{1-x}, N_x)

The microstructure of WC–Co–(Ti, M)(C_{1-x}, N_x) cemented carbides sintered at 1420 °C for 1 h was observed using BSE in SEM, as shown in Fig. 3. Core–rim structure is not observed when no solid solution was added, i.e., WC–10Co (Fig. 3a). When solid solution (Ti, M)(C_{1-x}, N_x) was added, the hard metals have a weak core–rim structure, which has been commonly found in conventional cermets. The dominant phases are identified in the micrographs based on the contrast levels of each phase, which are WC, (Ti, M)(C_{1-x}, N_x) solid solution, and Co binder phase, respectively. The initial (Ti, M)(C_{1-x}, N_x) particles which are not completely dissolved during sintering normally appear as black cores. The grayish rim surrounding the dark core shares the same metallic elements as core, but the contents of Ti, Ta, Nb and W are different. The Co binder phase is observed along the hard phase boundaries, in which Ti, Ta, Nb and W are also detected. In addition, some pores can be seen in the solid-solution-containing samples.

As shown in Fig. 3, it can be seen that the solid-solution (Ti, M)(C_{1-x}, N_x) addition has refining effects on the particle size of WC grain. In order to quantitatively analyze the particle size of WC, it was measured by standard intercept method, as plotted in Fig. 4. The average size of WC grains decreases from 0.73 to 0.60 μm with the solid-

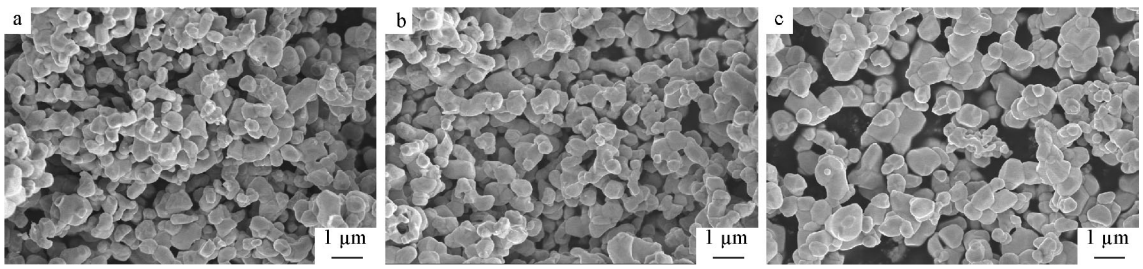

Fig. 2 SEM images of (Ti, M)(C_{1-x}, N_x) solid-solution powders with varied nitrogen contents: **a** $x = 0.15$, **b** $x = 0.20$, and **c** $x = 0.26$

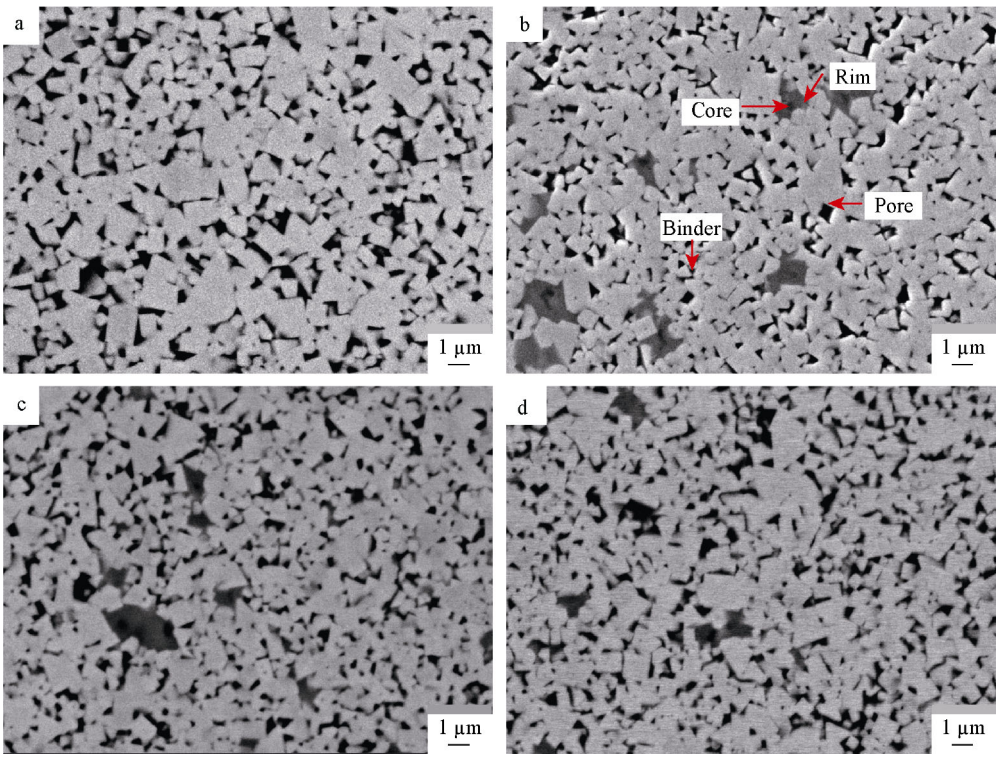

Fig. 3 BSE–SEM images of microstructure with various nitrogen contents: **a** Sample 1, **b** Sample 2, **c** Sample 3, and **d** Sample 4

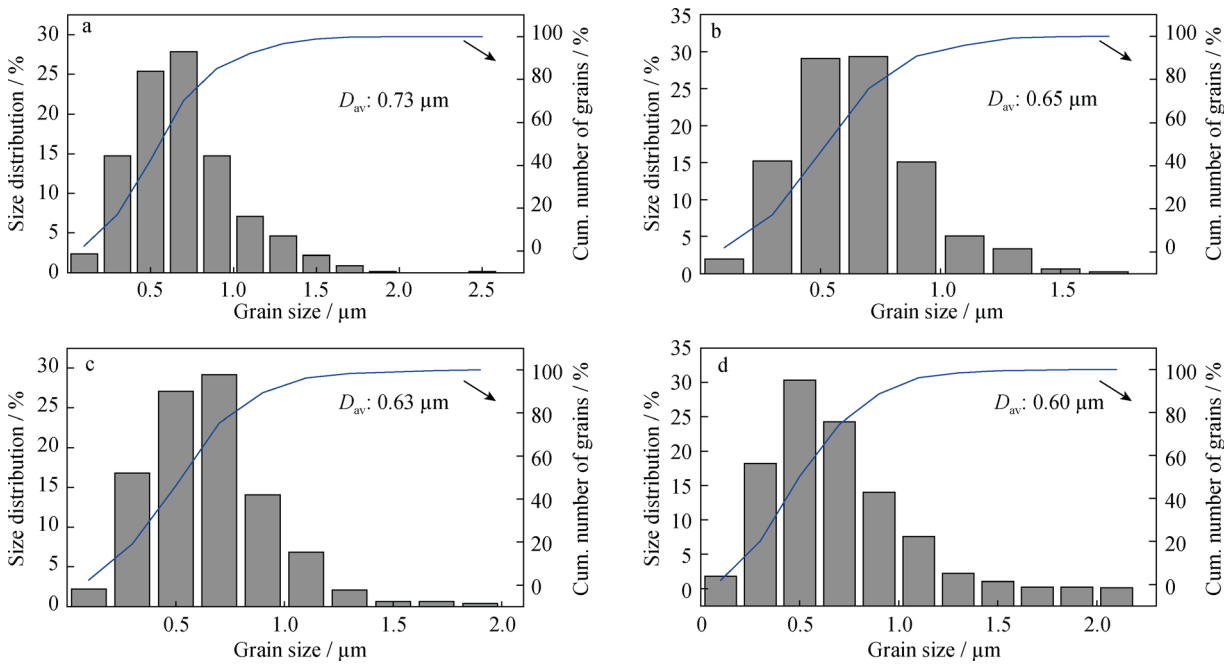

Fig. 4 Grain size distribution, cumulative (cum.) number of grains and average size (D_{av}) of **a** Sample 1, **b** Sample 2, **c** Sample 3 and **d** Sample 4

solution addition, and WC grains become faceted and the cobalt distribution gets more uniform. This is consistent with earlier observations that the sintered specimens manufactured from pre-alloyed raw materials have a homogeneous microstructure and have the effect of grain growth inhibitor [16]. The reasons for this phenomenon can be attributed to the classic sintering theories, Oswald ripening method. When the solid-solution powders were

added, with sufficient wetting of the molten liquid, the elements in solid-solution tend to be variable in the Co binder, which decreases the surface tension of solid/liquid interface and the solubility of WC in the melt. Hence, the dissolution–reprecipitation process during liquid-phase sintering is slowed down, and the coalescence and growth of the carbides are hindered. Therefore, addition of solid-solution powders can act as barriers to grain growth and lead to a uniform microstructure [17].

Furthermore, an interesting change is seen in the solid-solution-containing samples, as shown in Figs. 3 and 4. It is noted that the microstructure tends to refine with an increasing nitrogen content of the solid solution. On the one hand, this is due to the wettability between carbide particle and the metal binder. Igarashi et al. [18] found that there is a better wettability for Co with the increase in N/(C + N) ratio of solid solutions. Therefore, with the nitrogen content increasing in solid solution (Ti, M)(C_{1-x}, N_x), the wettability between Co and (Ti, M)(C_{1-x}, N_x) is enhanced, thereby inhibiting the coalescence of carbide particles. On the other hand, this may be controlled by the affinity of the constituent elements in the system. Previous work came to a conclusion that W has low affinity with nitrogen, especially in the NaCl (B1) structure [4]. It indicates that with the increase in nitrogen content, in this research system, the solubility of WC in the Co binder phase is reduced, the dissolution–reprecipitation process during liquid-phase sintering is slowed down, and the coalescence and growth of the carbides are hindered.

Although the microstructure of different samples has a similar appearance in Fig. 3, there is a gradual change in the core/rim structure with the variation in nitrogen content. From Fig. 3, it can be seen that the content of core–rim structure and the rim thickness decrease with the increase in nitrogen content in (Ti, M)(C_{1-x}, N_x) solid solution. The respective volume of cores and rims were determined by image analysis. The core contents of Samples 2, 3 and 4 are 0.38 vol%, 0.28 vol% and 0.22 vol%, and the core–rim contents are 2.34 vol%, 1.9 vol% and 1.46 vol%, respectively. That means with the increase in nitrogen content, the content of the rim decreases from 1.96 vol% to 1.24 vol%.

To illustrate this phenomenon, XRD analysis was carried out for the four samples with different nitrogen contents, as shown in Fig. 5. The analytical results show that the peaks are identified as three main phases corresponding to WC, (Ti, M)(C_{1-x}, N_x) and Co binder phase, and no new phase is formed. It is worth noting that the Bragg peaks for Co binder of Samples 2, 3 and 4 shift toward higher angles compared with that for Sample 1 (without solid-solution addition). It coincides with the above results of BSE–SEM that with the addition of solid solution (Ti, M)(C_{1-x}, N_x), the dissolution of WC particle in the Co binder phase is hindered, and

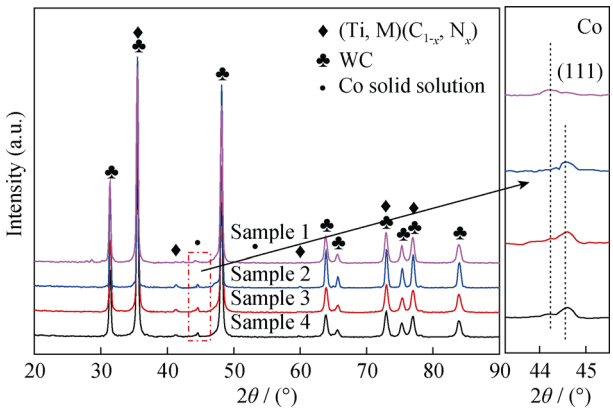

Fig. 5 XRD patterns of four samples with different nitrogen contents

thereby the lattice constant of Co turns to decrease, leading to that the Bragg peaks of Co binder shift toward higher angles compared with that of base specimen (Sample 1).

In addition, it is also found that the (111) peak of Co slightly shifts toward higher angles with the increase in nitrogen content of (Ti, M)(C_{1-x}, N_x) solid solution. It means that the increase in nitrogen content will result in the decrease of the lattice parameter of Co. And the decreased lattice parameter of Co binder phase will be intensified by the removal of M (Ta, Nb and W). In the light of previous work [19], it is known that the dissolution of heavy elements, such as Ta, Nb or W, is influenced by the melting point of the binder, which is closely related to the nitrogen content. Hence, it may be deduced that with nitrogen content increasing, the melting point of the Co binder rises, which exasperates the solubility of (Ti, M)(C_{1-x}, N_x) in the binder, and thus, the solution–precipitation processing is impeded. Therefore, the content of core–rim structure and the rim thickness decrease.

In order to further study the mechanism of variation in core–rim structure, the chemical compositions of the core–rim structure and the total content of Ti, Ta and Nb elements in core and rim versus the nitrogen content were analyzed by SEM–EDS, as shown in Table 2 and Fig. 6. The dissolution of Ti, Ta and Nb in the core phase increases with nitrogen content increasing, while that of the rim phase decreases. Clearly, the EDS results mean that as the nitrogen content increases, the dissolution of heavy elements in the rim phase is hindered and thus the rim thickness gets thinner, which corresponds well with the SEM results and the discussion above in the present study.

3.3 Mechanical properties

Micrographs of fractured surface and the crack propagating of Samples 1–4 are shown in Figs. 7 and 8. From Fig. 7, it can be seen that both transgranular and intergranular fractures exist, and the amount of intergranular fracture is

Table 2 EDS results of element content of core–rim structure (wt%)

Samples	Core					Rim			
	Ti	Ta	Nb	W	N	Ti	Ta	Nb	W
2	14.84	14.08	7.09	47.36	0.60	17.02	16.21	8.72	40.60
3	19.38	11.92	13.72	35.56	0.85	17.47	13.85	7.49	42.76
4	19.67	17.35	9.14	37.13	1.12	15.33	12.56	7.27	46.82

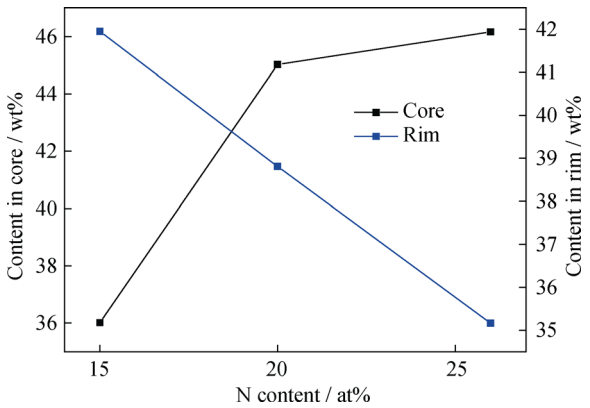

Fig. 6 Gross of Ti, Ta and Nb elements in core–rim structure

higher than that of transgranular fracture in all the four alloys and decreases with the nitrogen content increasing. It indicates that the crack propagation increasingly occurs in the binder phase which has a good plasticity, and this can be confirmed by the propagation path of crack, as shown in Fig. 8.

The mechanical properties of alloys depend not only on the compositions but also on the microstructural features [20]. The effect of nitrogen content on the relative density, transverse rupture strength (TRS), Vickers hardness and fracture toughness was measured at room temperature, as shown in Fig. 9.

The relative density of the four samples is presented in Fig. 9a. It can be seen that the relative density of solid-solution-containing samples are much lower than that of Sample 1 (without (Ti, M)(C_{1-x}, N_x) addition). Earlier study showed that the maximum densification is affected by contact angle, particle size, solubility of the solid in liquid, etc [21]. As (Ti, M)(C_{1-x}, N_x) solid solution dissolves in the binder and reprecipitates on the undissolved

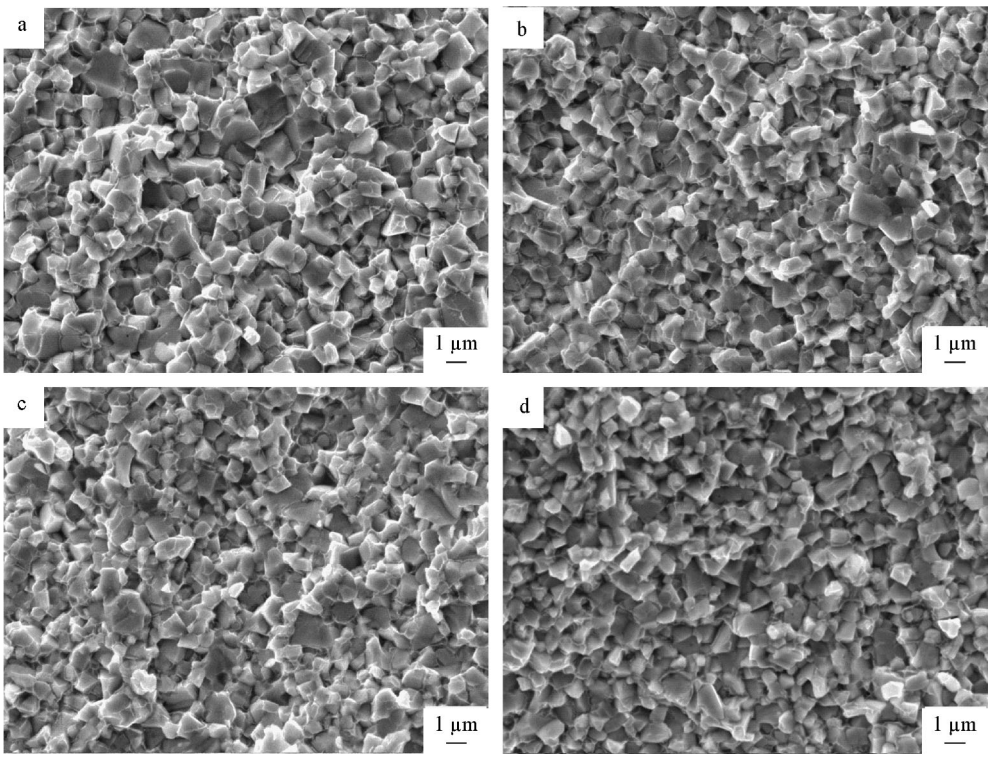

Fig. 7 Second electron (SE)–SEM images of fracture surfaces with different nitrogen contents: **a** Sample 1, **b** Sample 2, **c** Sample 3, and **d** Sample 4

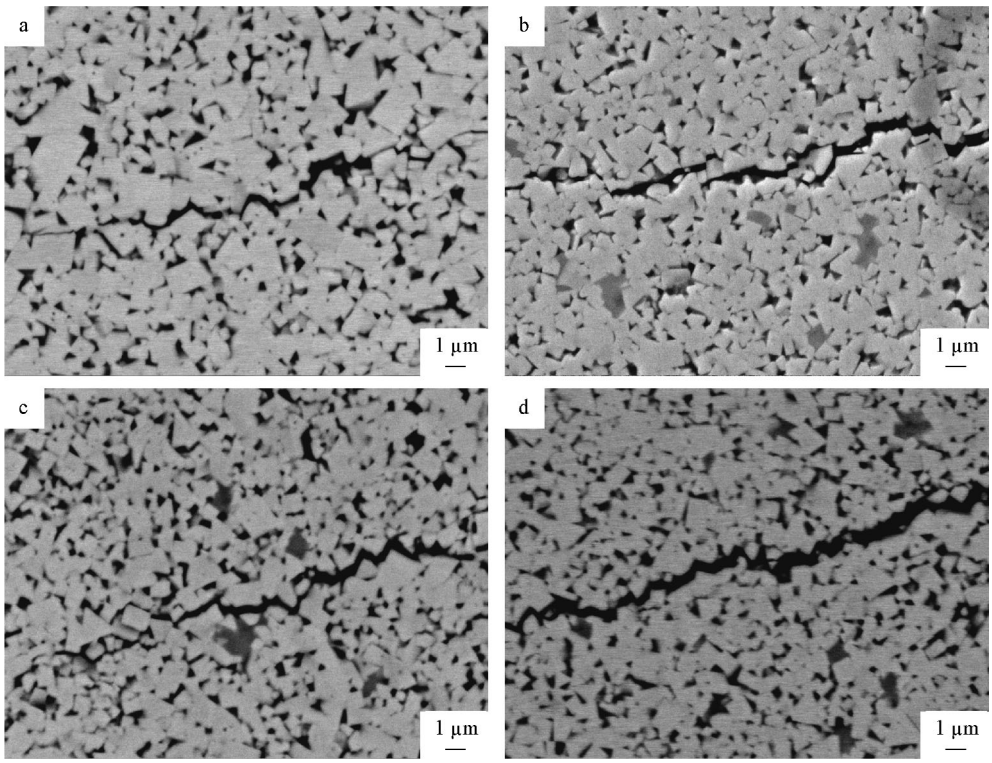

Fig. 8 SEM images of crack propagation of four samples with different nitrogen contents: **a** Sample 1, **b** Sample 2, **c** Sample 3, and **d** Sample 4

raw powders in the process of sintering, these solid solutions deteriorate the wettability between Co binder phase and hard phase. Hence, the addition of (Ti, M)(C_{1-x}, N_x) worsens the densification of WC–Co–(Ti, M)(C_{1-x}, N_x) cemented carbides.

In addition, with an increasing amount of nitrogen content in (Ti, M)(C_{1-x}, N_x), the relative density of the samples shows a decreasing tendency. The reason is due to the combined action of wettability between (Ti, M)(C_{1-x}, N_x) and Co binder phase and variation in liquid-phase content during the sintering process. As discussed above, Igarashi et al. [18] found that there is a better wettability for Co with the increase in N/(C + N) ratio of solid solutions. Densification requires a low contact angle to ensure that grains are pulled together. The relative good wetting of (Ti, M)(C_{1-x}, N_x) with higher nitrogen content makes the density increase. On the other hand, it is deduced that the melting point of Co binder rises with the nitrogen content increasing. It means that the content of Co liquid phase with high nitrogen (Ti, M)(C_{1-x}, N_x) addition decreases, thereby the binder phase could not thoroughly wet the hard phase and the pores cannot be sufficiently filled up; therefore, the relative density turns to decrease. In conclusion, under the condition of combined action, the relative density of the samples has a descending tendency.

It can be clearly seen in Fig. 9b that the TRS values of solid-solution-containing samples are much lower than that of Sample 1, the alloy free of solid solution. For Samples 2–4, the TRS values increase with the nitrogen content of (Ti, M)(C_{1-x}, N_x) solid solution increasing. These phenomena could be explained by the following factors: (1) the solid solution is a brittle-natured phase, which is confirmed to deteriorate TRS by working as fracture initiator when it locates close to the load; (2) the grain size refinement with nitrogen content increasing results in the improvement of TRS due to the Hall–Petch formula; and (3) with the decrease in the heavy element content in binder phase which promotes the plastic nature of the binder phase, the TRS values increase.

The hardness of the four samples is presented in Fig. 9c. The hardness of the samples firstly increases with the increase in nitrogen content, reaches a peak value at 20 at% nitrogen content and then decreases with the further increase in nitrogen content. This phenomenon can be explained by the following explanations. On the one hand, as the nitrogen content increases, the grain size slightly reduces. The hardness is influenced by the particle size, according to the Hall–Petch formula, and with the particle size decreasing, the hardness increases. As for the hardness, the peak value is achieved at 20 at% nitrogen at which the particle size is not the finest. It may be closely associated with the thickness of the rim phase. Previous research reported that the thickness distinctly influences the mechanical properties of the cermets [22]. It is noted that,

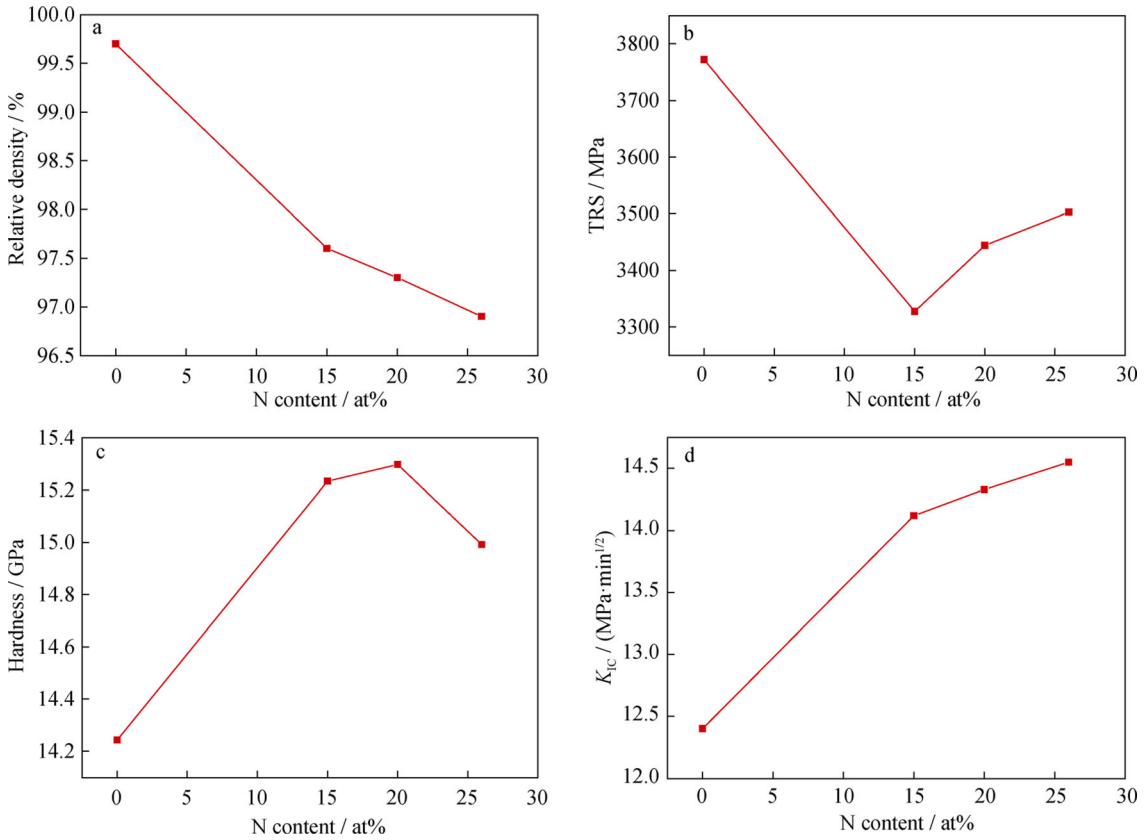

Fig. 9 Effect of nitrogen content on mechanical properties of four alloys: **a** relative density, **b** transverse rupture strength (TRS), **c** hardness, and **d** fracture toughness (K_{IC})

when the nitrogen content is 15 at%, the thickness of the rim is too thick, which turns to deteriorate the mechanical properties. However, when the nitrogen content is 26 at%, the rim is to some extent not intact, which will influence the wettability between core and the binder, leading the mechanical properties to be down. Therefore, the highest hardness value is found at the nitrogen content of 20 at%, which is characterized by fine grains and moderate thickness of rim phase.

Effect of nitrogen content on fracture toughness (K_{IC}) is plotted in Fig. 9d. Fracture toughness has an obvious promotion with nitrogen addition, but the improvement is not obvious when the nitrogen content increases. This result is in coherence with the following explanations. The fracture toughness depends on the flow stress and strain to rupture of the ligaments. With the increase in nitrogen content, the decrease in heavy element dissolved in the binder retards a hardening of the metal owing to solution hardening. Therefore, the flow stress of Co binder decreases with the nitrogen content increasing, leading to that the fracture toughness presents an ascending trend [23].

4 Conclusion

The effect of nitrogen content on the microstructure and mechanical properties of WC–10Co–1(Ti, Ta, Nb, W)(C_{1-x}, N_x) system cemented carbides were systematically investigated. The nitrogen content in the (Ti, Ta, Nb, W)(C_{1-x}, N_x) has a strong influence on the core–rim structure and composition. As the nitrogen content increases, the microstructure has a trend to become finer and the thickness of rim decreases with the increase in nitrogen content. The effects of nitrogen content on the mechanical properties of samples are obvious. The transverse rupture strength and the fracture toughness increase with nitrogen content increasing. The hardness firstly increases, reaches a peak at 20 at% nitrogen and then slightly decreases.

Acknowledgments This work was financially supported by the National Important and Special Project of China (No. 2013ZX04009-022) and Sichuan Provincial Science Research Program of China (No. 2013GC0136). We also acknowledge Analytical and Testing Center at Sichuan University for providing experimental facilities.

References

[1] Guo ZX, Xiong J, Yang M, Jiang CJ. WC–TiC–Ni cemented carbide with enhanced properties. J Alloys Compd. 2008; 465(1–2):157.

[2] Weidow J, Zackrisson J, Jansson B, Andrén H-O. Characterisation of WC–Co with cubic carbide additions. Int J Refract Met Hard Mater. 2009;27(2):244.

[3] Wu X, Guo ZM, Wang HB, Song XY. Mechanical properties of WC–Co coatings with different decarburization levels. Rare Met. 2014;33(3):313.

[4] Rafiaei SM, Kim JH, Kang S. Effect of nitrogen and secondary carbide on the microstructure and properties of $(Ti_{0.93}W_{0.07})$C–Ni cermets. Int J Refract Met Hard Mater. 2014;44:123.

[5] Liu C, Lin N, He YH, Wu CH, Jiang Y. The effects of micron WC contents on the microstructure and mechanical properties of ultrafine WC–(micron WC–Co) cemented carbides. J Alloys Compd. 2014;594:76.

[6] Li Y, Liu N, Zhang XB, Rong CL. Effect of carbon content on the microstructure and mechanical properties of ultra-fine grade (Ti, W)(C, N)–Co cermets. J Mater Process Technol. 2008; 206(1–3):365.

[7] Duman D, Gökçe H, Çimenoğlu H. Synthesis, microstructure, and mechanical properties of WC–TiC–Co ceramic composites. J Eur Ceram Soc. 2012;32(7):1427.

[8] Hashe NG, Neethling JH, Berndt PR, Andrén H-O, Norgren S. A comparison of the microstructures of WC–VC–TiC–Co and WC–VC–Co cemented carbides. Int J Refract Met Hard Mater. 2007;25(3):207.

[9] Chen X, Xiong WH, Qu J, Yang QQ, Yao ZH, Huang YZ. Microstructure and mechanical properties of (Ti, W, Ta) C–*x*Mo–Ni cermets. Int J Refract Met Hard Mater. 2012;31:56.

[10] Lindahl P, Rosén AE, Gustafson P, Rolander U, Andrén H-O. Effect of pre-alloyed raw materials on the microstructure of a (Ti, W)(C, N)–Co cermet. Int J Refract Met Hard Mater. 2000; 18(6):273.

[11] Park S, Kang S. Toughened ultra-fine (Ti, W)(CN)–Ni cermets. Scr Mater. 2005;52(2):129.

[12] Peng Y, Miao HZ, Peng ZJ. Development of TiCN-based cermets: mechanical properties and wear mechanism. Int J Refract Met Hard Mater. 2013;39:78.

[13] Shetty DK, Wright IG, Mincer PN, Clauer AH. Indentation fracture of WC–Co cermets. J Mater Sci. 1985;20(5):1873.

[14] Jin YZ, Liu Y, Wang YK, Ye JW. Synthesis of ultrafine (Ti, W, Mo, V)(C, N)–Ni composite powders by low-energy milling and subsequent carbothermal reduction–nitridation reaction. J Alloys Compd. 2009;486(1–2):L34.

[15] Zhang GP, Xiong WH, Yang QQ, Yao ZH, Chen S, Chen X. Effect of Mo addition on microstructure and mechanical properties of (Ti, W)C solid solution based cermets. Int J Refract Met Hard Mater. 2014;43:77.

[16] Hashe NG, Norgren SM, Andrén H-O, Neethling JH. Characterization of WC–(W, V)C–Co made from pre-alloyed (W, V)C. Int J Refract Met Hard Mater. 2009;27(2):229.

[17] Zhu G, Liu Y, Ye JW. Influence of Ce–Co pre-alloyed powder addition on the microstructure and mechanical properties of Ti(C, N)-based cermets. Int J Refract Met Hard Mater. 2013;37:134.

[18] Igarashi T, Kobayashi M, Takatsu S. Effects of TiN on microstructure and properties of WC-based cemented carbides. In: Proceedings of International Conference on the Science of Hard Materials 2. Rhodes; 1986. 12.

[19] Chen LM, Walter L, Klaus D. Advances in modern nitrogen-containing hardmetals and cemets. Int J Refract Met Hard Mater. 2000;18(2–3):153.

[20] Córdoba JM, Chicardi E, Gotor FJ. Development of multicomponent–multiphase materials based on (Ti, Ta, Nb)C_xN_{1-x} carbonitride solid solutions. Chem Eng J. 2012;192:58.

[21] Upadhyaya GS. Materials science of cemented carbides—an overview. Mater Des. 2001;22(6):483.

[22] Zhang Y, Zheng Y, Zhong J, Yuan Q, Wu P. Effect of carbon content and cooling mode on the microstructure and properties of Ti(C, N)-based cermets. Int J Refract Met Hard Mater. 2009; 27(6):1009.

[23] Shi ZM, Zhang DY, Chen S, Wang TL. Effect of nitrogen content on microstructures and mechanical properties of Ti(C, N)-based cermets. J Alloys Compd. 2013;568:68.